Electronic Supplementary Information (ESI)

Macroscopic Porous MnO_2 Aerogels for Supercapacitor Electrodes

Kongliang Xu,[a]† Xuedong Zhu,[b]† Ping She,[a] Yinxing Shang,[a] Hang Sun*[a] and Zhenning Liu*[a]

[a] Key Laboratory of Bionic Engineering (Ministry of Education), College of Biological and Agricultural Engineering, Jilin University, Changchun, Jilin 130022, P. R. China.
E-mail: sunhang@jlu.edu.cn; liu_zhenning@jlu.edu.cn
[b] College of Life Sciences, Jilin University, Changchun, Jilin 130022, P. R. China.
† These authors contributed equally to the work.

1. Experimental Section

1.1 Synthesis of the ultrathin MnO_2 nanosheets

$KMnO_4$ (A.R., Beijing Chemical Factory), sodium dodecyl sulfate (SDS, C.P., Tianjin Guangfu Fine Chemical Research Institute), concentrated hydrochloric acid (HCl, A.R., Beijing chemical factory) were purchased and directly used without further treatment or purification. Ultrathin MnO_2 nanosheets were prepared through the redox reaction between $KMnO_4$ and SDS. Briefly, SDS solution (100 mM, 32 mL), HCl solution (100 mM, 3.2 mL), $KMnO_4$ solution (50 mM, 3.2 mL) and 281.6 mL ultrapure water were mixed together and heated at 95 °C for 3 hours to form a brown flocculent precipitate. The precipitates were filtered and washed with ultrapure water and alcohol for multiple times, and then sonicated at 100 W to yield a colloidal solution of monodispersed ultrathin MnO_2 nanosheets.

1.2 Preparation of the self-standing MnO_2 aerogels

Self-standing MnO_2 aerogels were prepared by assembling the ultrathin MnO_2 nanosheets into 3D interconnected architectures via ice-templating and subsequent freeze-drying. Briefly, MnO_2 nanosheet colloids with a concentration of ~1 mg mL^{-1} were poured into a glass mold, which were then frozen at -20 °C for 12 hours to form icy chunks. Subsequently, the obtained frozen samples were directly transferred to a freeze-drier and freeze-dried at -50 °C for 24

hours to prepare self-standing MnO_2 aerogels. For comparison, the powder MnO_2 was prepared by directly drying of MnO_2 colloids at 90 °C.

1.3 Electrode preparation and electrochemical measurement

A three-electrode system with 1 M Na_2SO_4 aqueous solution as the electrolyte was set up to characterize the properties of the MnO_2 aerogels, where a platinum wire and the AgCl/Ag electrode (saturated with KCl) were used as the counter electrode and reference electrode, respectively. The working electrode was prepared by mixing 70 wt% active material (MnO_2 aerogels), 20 wt% acetylene black and 10 wt% polyvinylidene fluoride (PVDF) in N-methyl-2-pyrrolidone (NMP) and the slurry was daubed onto a nickel foam current collector (5 mm × 5 mm). The electrode was heated at 110 °C for 12 h to evaporate the solvent and then pressed under 10 MPa. The typical mass of the active material (MnO_2 aerogels alone) in the working electrodes was about 4 mg cm^{-2}. The control electrochemical measurement was carried out under the same condition using powder MnO_2 instead of MnO_2 aerogels.

The specific capacitance of the electrode is calculated from the cyclic voltammetry curve using the following equation:

$$C=(\int I\, dt) / (m\, \Delta V),$$

where C (F g^{-1}) is the specific capacitance, I (A) is the oxidation or reduction current, *dt* (s) is the time differential, m (g) is the mass of the active material, and ΔV (V) is the voltage of one sweep segment.

The specific capacitance of the electrode is also calculated from the galvanostatic discharge curve using the following equation:

$$C = (I\, \Delta t) / (m\, \Delta V),$$

where C (F g^{-1}) is the specific capacitance, I (A) is the constant discharge current, Δt (s) is the the discharge time, m (g) is the mass of active material in the electrode, and ΔV (V) is the potential window.

2. Figures

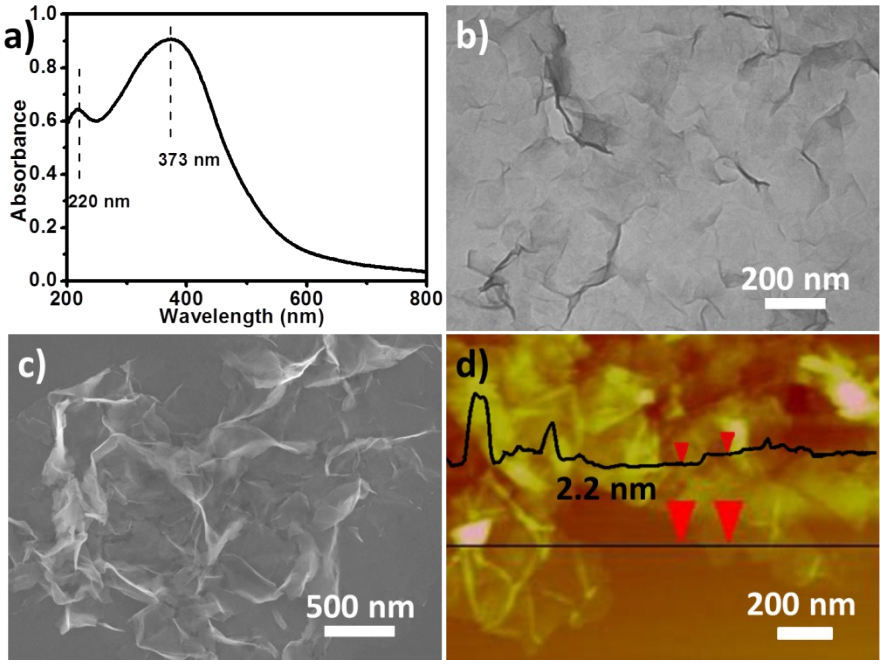

Fig. S1 Characterization of MnO_2 nanosheets: a) UV−vis absorption spectrum; b) TEM image; c) SEM image; d) AFM image and the height profile along the black line (the height measured between two red arrows is approximately 2.2 nm).

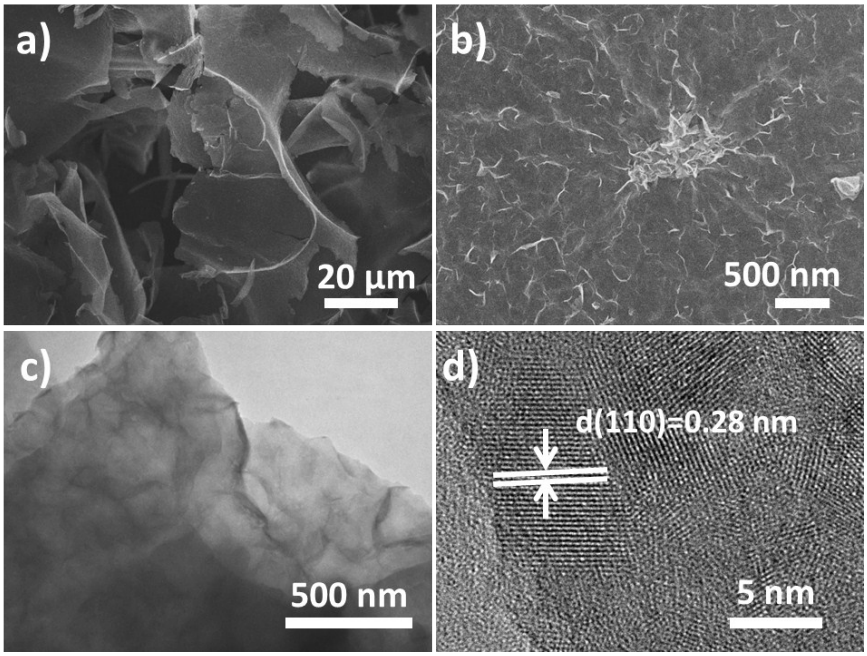

Fig. S2 a) SEM image of the obtained MnO_2 aerogel; b) SEM image of the MnO_2 aerogel at higher magnification; c) TEM image of the MnO_2 aerogel; d) HR-TEM image of the MnO_2 aerogel showing that the obtained MnO_2 aerogels are polycrystalline and the *d*-spacing of 0.28 nm revealed by lattice fringes corresponds to the *d*-value of the (110) plane of δ-MnO_2.

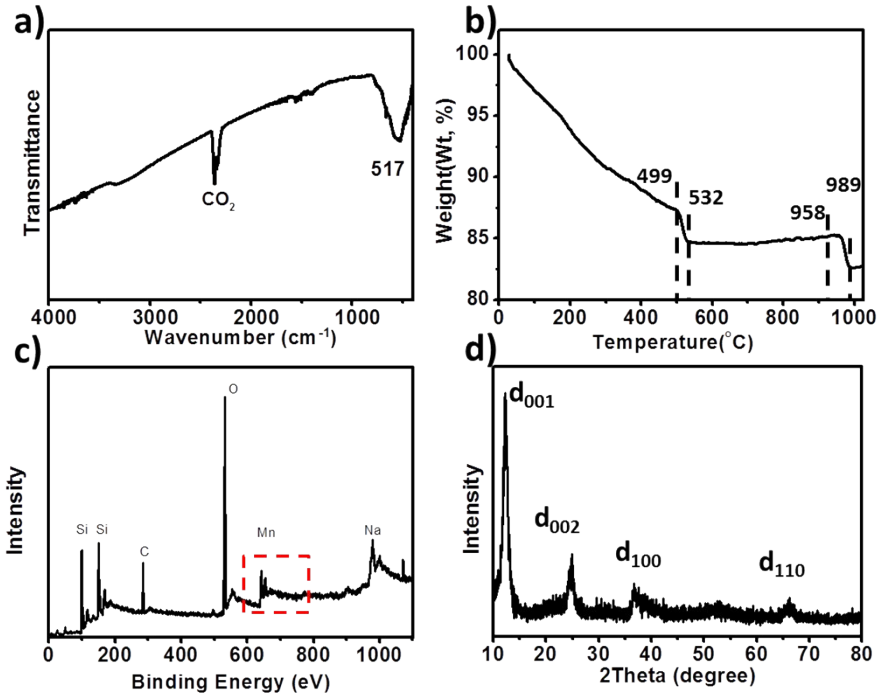

Fig. S3 a) FT-IR spectrum of the MnO_2 aerogels. The band at 517 cm^{-1} can be assigned to the vibrations of octahedral [MnO_6] framework. b) TGA curve of the MnO_2 aerogels. The weight loss before 499 °C can be attributed to the loss of surface and interlayer water, whereas the weight losses from 499 °C to 532 °C and 958 °C to 989 °C are probably caused by the transformations of MnO_2 to Mn_2O_3 and Mn_2O_3 to Mn_3O_4 respectively. c) XPS spectrum of the MnO_2 aerogels. The two peaks in the red box, centered at 642.0 eV and 653.9 eV, correspond to $Mn_{2p3/2}$ and $Mn_{2p1/2}$ of MnO_2 respectively. d) XRD profile of the MnO_2 aerogels exhibiting four peaks at 2θ=12.1°, 24.2°, 36.7°, 66.0°, which are in line with the characteristic peaks of *δ*-MnO_2 (JCPDS No. 18-0802).

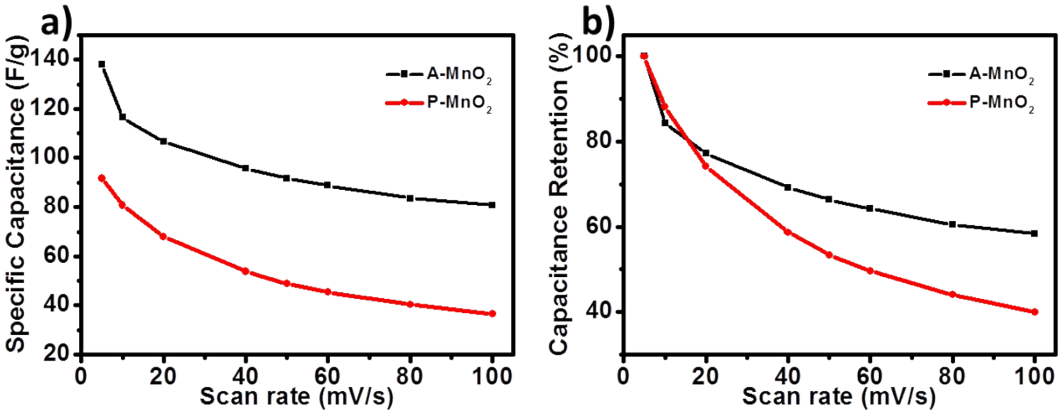

Fig. S4 a) Comparison of specific capacitance between A-MnO_2 and P-MnO_2 at various scan rates; b) comparison of capacitance retention (normalized to the capacitance at 1 A g^{-1}) between A-MnO_2 and P-MnO_2 at different scan rates.

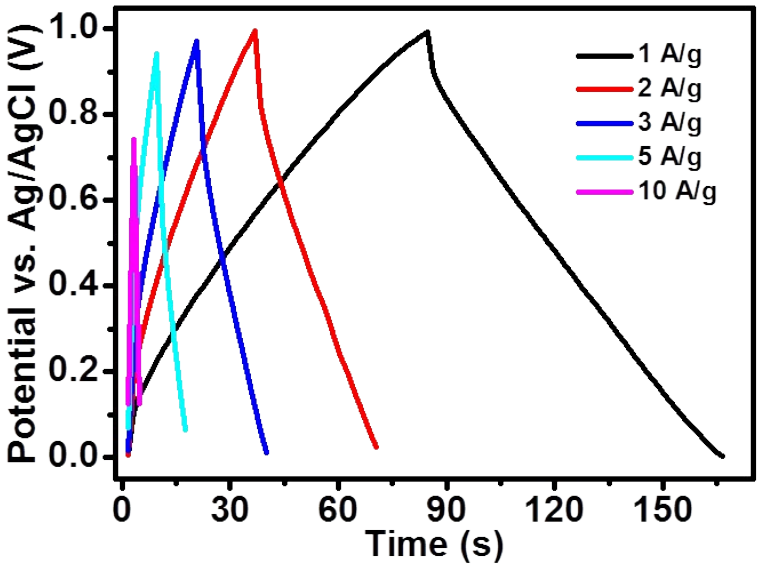

Fig. S5 Galvanostatic charge/discharge curves of P-MnO_2 at different current densities.

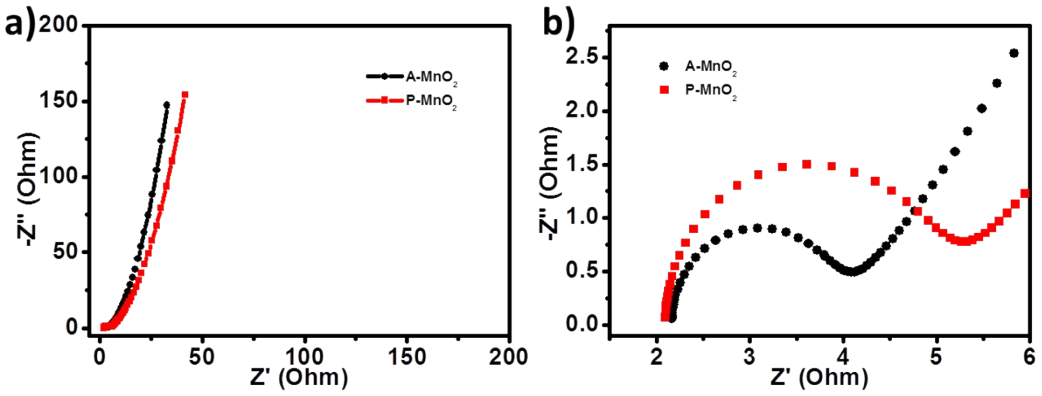

Fig. S6 Fitted Nyquist plots for A-MnO_2 (black lines) and P-MnO_2 (red lines) electrodes. (b) is the enlargement of (a) in the high frequency.

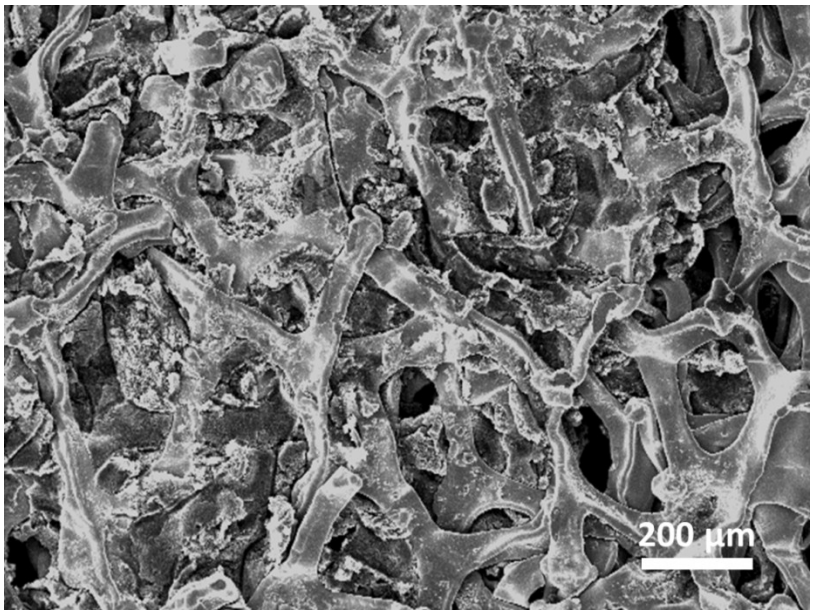

Fig. S7 SEM image of the MnO_2 aerogel electrode after being pressed at 10 MPa.

Table S1. Supercapacitive properties of MnO_2 based electrodes reported in recent literature

Morphology	**SC (F g^{-1})**	**Rate capability**	**Cycling durability**	**Reference**
MnO_2 nanosheets	1017 (3 mV s^{-1})	24% (3 to 50 mV s^{-1})	Unmentioned	1
MnO_2 nanosheets	868 (3 A g^{-1})	Unmenntioned	91% (10000 cycles)	2
MnO_2 nanosheet clusters	521.5 (5 mV s^{-1})	8% (5 to 50 mV s^{-1})	120% (1000 cycles)	3
MnO_2 nanolamellas	149.7 (2 A g^{-1})	72.6% (0.15 to 2 A g^{-1})	90% (3000 cycles)	4
MnO_2 nanowire array	493 (4 A g^{-1})	17 % (4 to 20 A g^{-1})	97.3% (800 cycles)	5
MnO_2 nanowire network	279 (1 A g^{-1})	54.5 % (1 to 20 A g^{-1})	97.3% (1000 cycles)	6
MnO_2 nanorods	120 (5 mV s^{-1})	57% (1 to 100 mV s^{-1})	Unmentioned	7
MnO_2 nanowires	108 (0.77 A g^{-1})	60% (0.077 to 0.77 A g^{-1})	88% (3000 cycles)	8
Porous MnO_2	218 (0.1 A g^{-1})	70.6 % (0.1 to 15 A g^{-1})	90% (4000 cycles)	9
MnO_2 nanoflowers	121.5 (1 mV s-1)	Unmentioned	71% (500 cycles)	10
Clewlike MnO_2	120 (5 mV s^{-1})	70% (5 to 200 mV s^{-1})	Unmentioned	11
MnO_2 nanoflowers	103.5 (0.5 A g^{-1})	64 % (0.5 to 10 A g^{-1})	120% (5000 cycles)	12
MnO_2/Carbon Aerogels	456 (5 mV s^{-1})	64 % (1 to 40 mV s^{-1})	97% (1000 cycles)	13
MnO_2-graphene aerogels	128 (2 A g^{-1})	47 % (0.5 to 6 A g^{-1})	99% (800 cycles)	14
MnO_2 carbonaceous aerogels	123.5 (5 mV s^{-1})	48 % (5 to 100 mV s^{-1})	60% (1000 cycles)	15
MnO_2-dispersed carbon aerogels	78 (5 mA.cm^{-2})	Unmentioned	Unmentioned	16
MnO_2 aerogels	139 (1 A g^{-1})	72.7 % (1 to 20 A g^{-1})	93.3% (5000 cycles)	Our work

Notes and references

1. G. X. Zhao, J. X. Li, L. Jiang, H. L. Dong, X. K. Wang and W. P. Hu, *Chem. Sci.*, 2012, **3**, 433-437.
2. Z. Liu, K. Xu, H. Sun and S. Yin, *Small*, 2015, **11**, 2182-2191.
3. Z. P. Feng, G. R. Li, J. H. Zhong, Z. L. Wang, Y. N. Ou and Y. X. Tong, *Electrochem. Commun.*, 2009, **11**, 706-710.
4. S. Chen, J. W. Zhu and X. Wang, *ACS Nano*, 2010, **4**, 6212-6218.
5. C. L. Xu, Y. Q. Zhao, G. W. Yang, F. S. Li and H. L. Li, *Chem. Commun.*, 2009, 7575-7577.
6. H. Jiang, T. Zhao, J. Ma, C. Y. Yan and C. Z. Li, *Chem. Commun.*, 2011, **47**, 1264-1266.
7. K. Kuratani, K. Tatsumi and N. Kuriyama, *Cryst. Growth Des.*, 2007, **7**, 1375-1377.
8. S. L. Chou, J. Z. Wang, S. Y. Chew, H. K. Liu and S. X. Dou, *Electrochem. Commun.*, 2008, **10**, 1724-1727.
9. X. Y. Xie, C. Zhang, M. B. Wu, Y. Tao, W. Lv and Q. H. Yang, *Chem. Commun.*, 2013, **49**, 11092-11094.
10. J. P. Ni, W. C. Lu, L. M. Zhang, B. H. Yue, X. F. Shang and Y. Lv, *J Phys. Chem. C*, 2009, **113**, 54-60.
11. P. Yu, X. Zhang, D. L. Wang, L. Wang and Y. W. Ma, *Cryst. Growth Des.*, 2009, **9**, 528-533.
12. W. Chen, R. B. Rakhi, Q. Wang, M. N. Hedhili and H. N. Alshareef, *Adv. Funct. Mater.*, 2014, **24**, 3130-3143.
13. G. R. Li, Z. P. Feng, Y. N. Ou, D. C. Wu, R. W. Fu and Y. X. Tong, *Langmuir*, 2010, **26**, 2209-2213.
14. C. C. Ji, M. W. Xu, S. J. Bao, Z. J. Lu, C. J. Cai, H. Chai, R. Y. Wang, F. Yang and H. Wei, *New J. Chem.*, 2013, **37**, 4199-4205.
15. Y. M. Ren, Q. Xu, J. M. Zhang, H. X. Yang, B. Wang, D. Y. Yang, J. H. Hu and Z. M. Liu, *ACS Appl. Mater. Inter.*, 2014, **6**, 9689-9697.
16. G. Lv, D. C. Wu and R. W. Fu, *J. Non-Cryst. Solids*, 2009, **355**, 2461-2465.